A NEW SHIP RECOVERY CONCEPT AND DESIGN USING ADAPTIVELY CONTROLLED BUOYANCY SYSTEMS

AKD Velayudhan[1], N Srinil[1], N Barltrop[1]

ABSTRACT

In this paper, attention is placed on the salvage of a sunken ship resting on the seafloor by introducing a new design concept based on the adaptively-controlled buoyancy (gas-inflating) systems. A mathematical model describing a ship rigid-body motion in a vertical diving plane accounting for the heave and pitch degrees of freedom will be presented and analyzed with respect to both hydrostatic and hydrodynamic loads. A new design approach is implemented by integrating a fuzzy logic algorithm with the sliding mode controller to bring together the advantages of both controllers. An adaptive fuzzy sliding-mode control strategy (Conventional or Two input fuzzy sliding mode controller and Single input fuzzy sliding mode controller) ensuring a safe and stable ascending ship dynamics will be presented along with the discussion of a practical aspect of automatic controller design regulating the gas inflating flow rate. Computational simulations with a series of parametric studies based on an experimental ship model will be carried out to show the effectiveness of the proposed adaptive fuzzy sliding mode controllers and its comparative performance with conventional sliding mode controller. It is found that both fuzzy sliding mode controllers show about 30 % of improvement in tracking performance over the conventional controller in which single input fuzzy sliding mode controller is the optimum choice due to less tuning effort and computational time.

KEY WORDS

Marine Salvage; Buoyancy Systems; Breakout Force; Two Input & Single Input Fuzzy Sliding Mode Controller.

INTRODUCTION

As far as marine salvage operation is concerned literature sources reporting systematic data and information useful for system modeling are relatively few. Studies regarding the dynamics of salvage operation are of course complicated by the fact that, in addition to the influence of complicated hydrodynamic forces and moments and breakout forces, the external disturbances and uncertainty are to be taken in to account. There are three methods commonly used in the marine salvage industry to extract the sunken objects from the sea bottom, i.e. by using the floating cranes, the Remotely Operated Vehicles (ROVs) and the buoyancy systems. Floating cranes can be used for water depths of 2000 m with a good controllability; however the weight of cables becomes more than that of the payload for deeper lifts and hence the process becomes awkward and costly. As the cranes are fitted onto a moving vessel, there will be the operational constraints due to the limiting sea state affected by weather conditions. Excessive cost of hiring and the limited availability of cranes are the major problems facing the salvage industry. ROVs, on the other hand, can be used in higher water depths and they are highly controllable. Nevertheless, they can be only used for lifting smaller objects as the lifting capacity is limited by the size and power of the thrusters used for the propulsion (Nicholls-Lee, et al 2009). As an advantage, buoyancy systems can be used for lifting any size of objects from any depths with comparatively less costs.

The concept of using a buoyancy system (e.g. the gas inflated bags) for salvaging sunken vessels from the deep ocean has been around for centuries. This operation is based on the well-known 'Archimedes' principle for which the force on the object can be determined by subtracting the dry weight of the object from the weight of the fluid displaced by that object (Rawson & Tupper 2001). In general, the bottoms of inflatable bags (e.g. balloons) are attached to the payload to be lifted and inflated using pipes from the gas generating system. The main drawback of using the inflating bags for marine salvage operation is due to the difficulty in controlling the vertical speed as the ship ascends. A large buoyancy force may be initially

[1] Department of Naval Architecture & Marine Engineering, University of Strathclyde, Glasgow UK

required to separate the ship from the seabed, resulting in an excessive vertical speed. During the ascent, any trapped air inside the hull may also expand and further increase the buoyancy; thus the balloons themselves may slightly expand as the hull ascends. Excessive speed will result in a potentially-hazardous working environment to divers and salvaging crews and this may cause the lifting bag to breach the surface of the water so fast that the air escapes from the bottom. This purge cause the payload to sink back to the bottom which, in turn, results in a loss of time, damage to the hull, high operating and maintenance costs, and the risk to divers and crew members (Farrell & Wood 2009; JW Automarine 2010). Open bottom bags dump excess gas from the bottom during the ascent whereas enclosed lift bags only have a limited capacity to dump excess gas through the pressure release valves (Nicholls-Lee, et al 2009).

Hence, an automatic controller is required to regulate the volume flow rate of filling gas inside the balloon (i.e. the pump flow rate) along with pressure release valves to ensure a safe and steady ascent. Purge valves can be controlled either mechanically (spring loaded) or electrically (Farrell & Wood 2009). Because of the attractive advantages, a sliding mode controller is selected initially to regulate the pump flow rate (Slotine & Li 1991). In a sliding mode controller, the states switch between the stable and unstable trajectories until the state variables reach the sliding surface. The phase trajectory of a sliding mode controller can be divided into two stages: the reaching and the sliding mode. Reaching or hitting phase is the trajectory starting from the given initial conditions of the sliding surface and tending towards the sliding surface; then the sliding mode starts once the state variables converge to the sliding surface. When the state variables are in the sliding mode, the system remains on the sliding surface and the states go the origin while the system is insensitive to parameter variations or external disturbances. That is the controller works effectively in the sliding mode. On the contrary, when the system acts in the reaching mode, tracking errors cannot be directly controlled, hence the system becomes sensitive to parameter variations. This implies that the robustness of the sliding mode controller resides in its sliding phase rather than the reaching phase, owing to the fact that the conventional sliding mode controllers uses fixed (invariant) sliding surfaces. Conventional sliding mode controllers with predetermined fixed slope (λ) degrade the dynamic performance of the system during the reaching mode. I.e. the controllers with minimum values of slope (λ_{min}) lead to a slower error convergence but better tracking performance, whereas controllers with maximum values of slope (λ_{max}) lead to a faster error convergence along which the tracking accuracy can be degraded. In addition, finding the optimum value of slope for the given controller is a complicated task (Yorgancioglu & Komurcugil 2010). Thus, it is a very important task in sliding mode controller design is to continuously change the slope of the sliding surfaces based on the state errors and their derivatives. This task is accomplished by using a Fuzzy Logic Controller (FLC) that continuously computes the slope of the sliding surface according to the values of state error and its derivatives. The chattering can also be effectively eliminated by this approach (Yagiz & Hacioglu 2005; Yorgancioglu & Komurcugil 2008; Eksin, et al 2002). Another difficulty faced by the control engineers in sliding mode controller is how to tune the controller effectively for a desired performance. Normally, this operation is carried out by a trial and error method being cumbersome and time consuming. A constant high value of controller gain often leads to the chattering. This problem can be overcome by adaptively tuning the controller by another FLC that computes the controller gain k based on the sliding surface σ and its variation (Huang, et al 2007; Bazzi & Chalhoub 2005; Guo & Woo 2003; Abdelhameed 2005). Hence, it is found that the performance of the conventional sliding mode controller can be effectively improved by using the FLC for continuously computing the slopes of the sliding surface instead of a constant sliding surface and also adaptively tuning the controller gain (k) by another FLC.

In this paper, a conventional or two input fuzzy sliding mode controller & single input fuzzy sliding mode controller are designed to improve the performance of the sliding mode controller. This paper is structured as follows. In Section 2, the dynamic equations of rigid-body motion describing a raising sunken vessel are formulated and presented in a state-space form. In Section 3, a conventional sliding mode-depth controller is designed based on the state space model and later it is extended to conventional and single input fuzzy sliding mode controllers. Numerical simulation results based on a pontoon experimental model are discussed in Section 4. The paper ends with the conclusions in Section 5.

PROBLEM FORMULATION

Forces acting on a sunken vessel consist of hydrostatic and hydrodynamic components. The variation of hydrodynamic forces with velocities, accelerations and control surface deflections are expressed in terms of hydrodynamic coefficients. These coefficients can be derived from physical model tests or theory, the number of coefficients used being subject to the amount of data available, past experience etc. The equations of motion presented here are the core of the simulation program. These equations, using body axes variables are solved for the motions in diving plane. These variables are then transformed to the earth–fixed coordinates using the kinematic relations. The system is then placed in state space form so that state space model can be formed simply by assigning states to the associated variables. The form of the force expressions presented here is currently used in computer programs in Matlab.

Model of a Raising Vessel

To describe the motion of a raising vessel, two reference frames are considered as in Figure 1, including the earth- and body-fixed frames. The origin of the body-fixed frame coincides with the centre of gravity (*Cg*) of the vessel when *Cg* is the principle plane of symmetry or at any other point if this is not the case (Fossen 1994; Fossen 2002; Healey & Lienard 1993). The positions and orientations of the vessel (kinematic variables) are expressed with respect to the earth-fixed coordinates whereas the linear and angular velocities of the vessel (dynamic variables) are expressed in the body-fixed coordinates. The transformation between the two coordinate systems is done by using Euler angles (Φ, θ, ψ).

To describe the dynamics of the sunken vessel ascending from the seafloor, it is preliminarily assumed that:

- the vessel behaves as a rigid body,
- the acceleration of a point on the surface of the earth is neglected,
- the external loads comprise of the breakout, hydrostatic and hydrodynamic drag forces, and the seabed is flat creating a breakout (lift) force of 1.3 times the ship wet weight.

Equations of Motion

As the problem is concerned with the dynamics of raising sunken vessels (i.e. the control surfaces are inactive and the depth control is by regulating the additional buoyancy provided by the inflating system), it is further assumed to consider only the diving vertical-plane (surge, heave and pitch) motions in the stability analysis. However, the surge motion couples with the heave and pitch motions through the meta-centric height. This dynamic coupling could be eliminated by redefining hydrodynamic coefficients with respect to the ship's Cg instead of its geometric centre (Healey & Macro 1992; Cristi, et al 1990). For a sunken vessel, it is also known that the forward speed is zero. However, due to external forces such as currents, the surge motion may exist. As sliding mode controller can effectively handle system modelling errors, external disturbances and uncertainty and thereby maintain hydrodynamic stability throughout the process so that in this study, we implement the sliding mode control strategy to the linear equations of motion with the neglected surge motion (Velayudhan, et al 2011). Thus, the system model variables include the heave velocity (*w)*, pitch angle (θ), pitch rate (q) and global depth position (z).

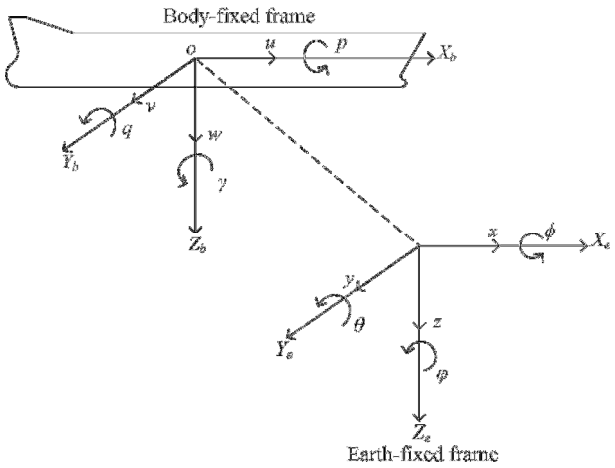

Figure 1: Motion variables for a marine vessel

Accordingly, the equations of motion for heave and pitch read (Fossen 1994)

$$m\left(\dot{w} - x_G\dot{q} - z_G q^2\right) = Z \quad [1]$$

$$I_{yy}\dot{q} + m\left[z_G(wq) - x_G\dot{w}\right] = M \quad [2]$$

where,

m	vessel mass (kg)
I_{yy}	mass moment of inertia (kg.m^2)
x_G ,z_G	coordinates of the centre of gravity in X and Z directions respectively
Z	heave force (N).
M	pitch moment (N.m)

Hydrostatic Force and Moment

Hydrostatic force and moment are due to the ship weight W and buoyancy B. The buoyancy of the sunken vessel may be changed due to the sea density variation and to the compressibility of the hull. Herein, the former case is accounted for through a linear volume change with depth,

$$B = \rho \nabla g + \mu z(\rho / \rho_O) \quad [3]$$

in which

μ	Increase in buoyancy per unit increase in depth in sea water of standard density ρ_o (N.m)
ρ	Actual density of surrounding sea (kgm^{-3})
∇	Volumetric form displacement (m^3)
g	Gravitational acceleration (ms^{-2})
z	Vertical coordinate position (m)

In the body-fixed coordinate system, the hydrostatic components of force and moment for heave/pitch motions are (Fossen 1994; Fossen 2002):

$$Z_{hs} = (W - B)\cos\theta \quad [4]$$

$$M_{hs} = -(z_G W - z_B B)\sin\theta - (x_G W - x_B B)\cos\theta \quad [5]$$

where

W	Vessel dry weight (N)
B	Buoyancy force (N)
θ	Pitch angle (deg.)
x_B , z_B	Coordinates of the centre of buoyancy in X and Z directions respectively

Hydrodynamic Force and Moment

The hydrodynamic components of force and moment for heave/pitch motions are (Fossen 1994; Healey & Lienard 1993):

$$Z_{hd} = \frac{1}{2}\rho \ell^3 Z'_{\dot{w}} \dot{w} + \frac{1}{2}\rho \ell^4 Z'_{\dot{q}} \dot{q} - \frac{1}{2}\rho C_D A_s w^2 \quad [6]$$

$$M_{hd} = \frac{1}{2}\rho \ell^4 M'_{\dot{w}} \dot{w} + \frac{1}{2}\rho \ell^5 M'_{\dot{q}} \dot{q} \quad [7]$$

in which

l	Vessel length (m)
$Z'_{\dot{w}}$	Added mass coefficient in heave
$Z'_{\dot{q}}$	Added mass coefficient in pitch
$M'_{\dot{w}}$	Added mass moment of inertia coefficient in heave
$M'_{\dot{q}}$	Added mass moment of inertia coefficient in pitch
C_D	Drag coefficient
A_s	Vessel surface area (m^2)

Let

$$Z_{\dot{w}} = \frac{1}{2}\rho l^3 (Z_{\dot{w}}'), \quad \dot{Z}_{\dot{q}} = \frac{1}{2}\rho l^4 (Z_{\dot{q}}') \qquad [8]$$

Consequently, Equation 6 may be simplified as

$$Z_{hd} = Z_{\dot{w}}\ \dot{w} + Z_q\ \dot{q} - \frac{1}{2}\rho C_D A_s w^2 \qquad [9]$$

Similarly, by letting

$$M_{\dot{w}} = \frac{1}{2}\rho l^4 (M_{\dot{w}}'), \quad M_{\dot{q}} = \frac{1}{2}\rho l^5 (M_{\dot{q}}') \qquad [10]$$

Therefore, Equation 7 may be simplified as

$$M_{hd} = M_{\dot{w}}\ \dot{w} + M_{\dot{q}}\ \dot{q} \qquad [11]$$

Breakout Force

The breakout or suction force accounts for the difference between the total lift force required and the object's wet weight. It is theoretically and empirically difficult to estimate this breakout force due to the involvement of several variables and unknowns (U.S. Navy 1992). In general, the amount of breakout force & estimation of break out time depends on the seafloor soil characteristics (i.e. the compressibility of soil skeleton and pore water, permeability etc.), the embedment depth and time, the object shape parameters and the loading conditions. The lift force (F) required for the complete extraction of the object from the sea bottom should be greater than their submerged weight (G) due to the ground reaction (R) exerted by the soil (Figure 2). Sawicki and Mierczynski (2003) proposed a simple formula for the estimation of lift force as $F = (1 + k_p)\ G$ where k_p is an empirical coefficient depending on the subsoil.

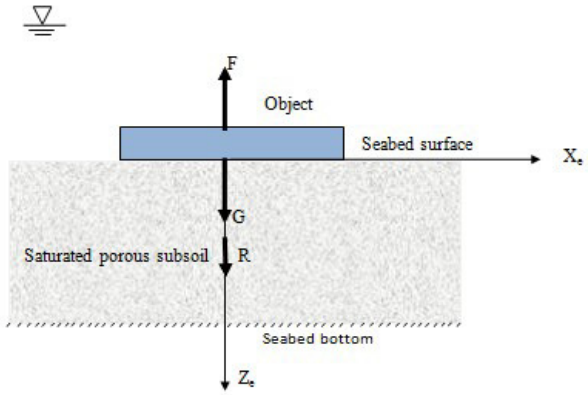

Figure 2: Lift force model to extract an object from the seabed (Sawicki and Mierczynski 2003)

Vaudrey (1972) investigated the efficacy of 3 analytical methods (i.e. Muga, Liu and Lee methods) for the prediction of breakout forces with different object shapes such as a cylinder, sphere and block, with and without breakout force reduction techniques. From the analysis, it was observed that the use of breakout reduction methods such as the mud suction tubes, water flooding and air jetting would reduce the total lift force by approximately 15% and eliminate the snap loading condition. The selection of breakout reduction methods depends on the particular salvage operation, bottom soil conditions and the availability of equipments. From the above literature, the total lift force is assumed to be 1.3 times the wet weight of the vessel. Break out time can be calculated based on the work of Mei et al (1985) & Foda (1982).

Additional Buoyancy by the Inflating System

For the sunken vessel resting on the seafloor, the vessel weight is balanced by both the buoyancy and the ground reaction (U.S.Navy 1992). Additional force required to lift the vessel should overcome both the in-water object weight and the ground reaction. This force, described in terms of the buoyancy, could be provided by the volume of gas inside the balloons. The gas-generating system (solid, liquid or cryogenic pressurised system) is used such that the produced gas is pumped into the balloons at a desired flow rate using pipes. During the ascent, a lift bag may experience a pressure decrease due to the depth variation. This decreased pressure makes the volume of gas inside the balloon increase or makes the lift bag expand, following the Boyle's law,

$$P_1V_1 = P_2V_2 \text{ or } V_2 = \frac{P_1V_1}{P_2} \quad [12]$$

where P_1 is the initial absolute pressure, V_1 the initial volume inside the lift bag, P_2 the final absolute pressure and V_2 the final volume inside the lift bag. Nevertheless, as the pressure relief valves are provided either mechanically (spring loaded) or electrically at the top of the lift bag to purge out the excess gas inside the balloon, a constant buoyancy could be maintained (Farrell & Wood 2009). The variation of volume with respect to the time during inflating process can be accounted for by considering the volume flow rate of filling gas inside the balloon (i.e. the control parameter) as follows:

$$\frac{dV}{dt} = \dot{V} = f \quad [13]$$

where *f is* the gas flow rate (m^3s^{-1}). Consequently, the additional buoyancy provided by the inflating system can be written as

$$B_a = (\rho - \rho_g)gV \quad [14]$$

Kinematic Relations

The kinematic relations are used to transform the motion variables from the local to global coordinate system (Fossen 1994; Fossen 2002). The simplified kinematic relations for heave and pitch motions are

$$\dot{z} = w\cos\theta \quad [15]$$

$$\dot{\theta} = q \quad [16]$$

State-Space Matrix Model

For small values of pitch angle, it is assumed that $\sin\theta = \theta$ and $\cos\theta = 1$. Imposing the linearization and neglecting the products of small motions, the equations of motion can be written in the state-space matrix form as

$$[M_0]\{\dot{x}_s\} = [A_0]\{x_s\} + [B_0]\{u_c\} \quad [17]$$

$$[M_0] = \begin{bmatrix} m - Z_{\dot{w}} & -mx_G - Z_{\dot{q}} & 0 & 0 & 0 \\ -mx_G - M_{\dot{w}} & I_{yy} - M_{\dot{q}} & 0 & 0 & 0 \\ 0 & 0 & 1 & 0 & 0 \\ 0 & 0 & 0 & 1 & 0 \\ 0 & 0 & 0 & 0 & 1 \end{bmatrix} \quad [18]$$

$$[A_0] = \begin{bmatrix} 0 & 0 & 0 & 0 & -(\rho_{water} - \rho_{gas})g \\ 0 & 0 & 0 & -(z_G W - z_B B) & (\rho_{water} - \rho_{gas})gx_B \\ 1 & 0 & 0 & 0 & 0 \\ 0 & 1 & 0 & 0 & 0 \\ 0 & 0 & 0 & 0 & 0 \end{bmatrix} \quad [19]$$

$$\{B_0\} = \begin{bmatrix} 0 \\ 0 \\ 0 \\ 0 \\ 1 \end{bmatrix} \{x_s\} = \begin{bmatrix} w \\ q \\ z \\ \theta \\ V \end{bmatrix} \quad u_c = f \quad [20\text{-}22]$$

where x_s is the state vector and u_c is the control vector.

Equation 17 can be reduced in the form

$$\{\dot{x}_S\} = [A]\{x_S\} + [B]\{u_C\} \quad [23]$$

which is the State Dependant Riccati Equation (SDRE) where [A] and [B] are the input matrices given by

$$[A] = [M_0]^{-1}[A_0],\ [B] = [M_0]^{-1}[B_0] \quad [24]$$

CONTROLLER DESIGN

Conventional Sliding Mode Controller (CSMC)

A sliding mode controller (SMC) is selected for regulating the volume flow rate of filling gas inside the balloons in order to maintain the stability of the raising vessel within the diving plane. This selection was made due to the following reasons (Healey & Macro 1992; Healey & Lienard 1993; Yoerger & Slotine 1985; Slotine & Li 1991):

- SMC compensates for nonlinear behaviours
- SMC provides robustness to uncertainty
- SMC is straightforward to implement

In a closed loop control system, the function of the controller is to make the state variable x_s follow the desired state x_d with a prescribed dynamic characteristic in the presence of uncertainty and disturbances. The state variable error is defined as

$$e = x_s - x_d \quad [25]$$

or in general, the state variable error vector can be written as

$$\tilde{e} = (e, \dot{e}, \ddot{e} \ldots . e^{(n-1)})^T \quad [26]$$

where n is the order of the system. In the development of sliding mode controller, a sliding surface (σ) is to be created from a linear combination of the state variable errors such as position, velocity and acceleration. The aim is to drive the system to the sliding surface and ultimately to the condition $\sigma = 0$ while making sure that the state variables are always reducing (Slotine & Li 1991; Healey & Lienard 1993; Healey & Macro 1992; McGookin 1997). The sliding surface σ can be defined for an n^{th} order system as

$$\sigma = \left(\frac{d}{dt} + \lambda \right)^{n-1} e \quad [27]$$

For a second order nonlinear system, the corresponding sliding surface would be defined as

$$\sigma = \lambda e + \dot{e} \quad [28]$$

where λ is the slope of the sliding surface. Then, the Lypunov method can be used to formulate the control law (u_c), which is further developed by defining a positive definite function , $V(\sigma) > 0$ where the derivative of this function for all times greater than zero is negative. By defining a positive definite Lyapunov function's derivative as negative, we guarantee that the sliding surface (σ) is always reducing (Slotine & Li 1991; Healey & Lienard 1993; Healey & Macro 1992; McGookin 1997).

Let the Lypunov function,

$$V(x_s) = \frac{1}{2}\left[\sigma(x_s)\right]^2 \quad [29]$$

The scalar function $\sigma(x_s)$ is the weighted sum of the errors in the states x_s.

$$\sigma(x_s) = s^T x_s \quad [30]$$

The time derivative of Lypunov function $V(x_s)$ should be negative in order to provide stability (Healey & Lienard 1993; Healey & Macro 1992),

$$\dot{V}(x_s) = \sigma\dot{\sigma} < 0 \quad [31]$$

This can be accomplished if

$$\sigma\dot{\sigma} = -\eta^2 |\sigma| \quad [32]$$

The term η^2 is an arbitrary positive quantity, selected to ensure that $\dot{V}$ is negative even in the presence of modeling errors and disturbances. Therefore

$$\dot{\sigma} = -\eta^2 \frac{|\sigma|}{\sigma} = -\eta^2 sgn(\sigma) \quad [33]$$

where $Sgn(\sigma)$ is the signum function that is discontinuous across the sliding surface provided to ensure stability and is given by (Healey & Lienard 1993; Healey & Macro 1992; McGookin 1997),

$$Sgn(\sigma) = \begin{cases} 1, & \text{if } \sigma > 0 \\ 0 & \text{if } \sigma = 0 \\ -1, & \text{if } \sigma < 0 \end{cases} \quad [34]$$

From Equations 30 and 23,

$$\dot{\sigma} = s^T \dot{x}_s = s^T \left[A x_s + B u_c \right] \quad [35]$$

Combining Equations 33 and 35, we can write

$$\dot{\sigma} = s^T \dot{x}_s = s^T \left[A x_s + B u_c \right] = -\eta^2 sgn(\sigma) \quad [36]$$

By solving the above equation, the control law u_c is obtained as

$$u_c = -\left[s^T B \right]^{-1} s^T A - \left[s^T B \right]^{-1} \eta^2 sgn(\sigma) \quad [37]$$

in which the first term describes the nonlinear state feedback whereas the second term represents the switching control law. A control law of the form (Equation 37) guarantees the stability for nonlinear systems whereas the discontinuous term (*sgn (σ)*) results in undesirable chattering around the sliding point. It can be avoided by smoothing the control law with in a thin boundary layer around the sliding surface. This can be achieved by choosing a boundary layer thickness Φ_b and replacing the discontinuous *signum* function by a continuous saturation *function* (*sat* (σ/Φ_b)) (Yoerger & Slotine 1985; Slotine & Li 1991; McGookin 1997). This *saturation* function has the same end points as the *signum* function, however the area the zero σ value has a gradual transition towards zero value as $\sigma \rightarrow 0$ (McGookin1997; Fossen 1997). Next, the control law u_c can be written after linearization and smoothing as,

$$u_C = -\left[s^T B\right]^{-1} s^T A x_S - \left[s^T B\right]^{-1} \eta sat\left(\sigma/\Phi_b\right) \quad [38]$$

Where

$$sat\left(\sigma/\Phi_b\right) = \begin{cases} \text{sgn}\ (\sigma) & |\sigma| > \Phi \\ \sigma/\Phi_b & |\sigma| \le \Phi \end{cases} \quad [39]$$

The values of A and B can be obtained from Equation 24. By further letting $k = [s^T B]^{-1} s^T A$, then the above equation becomes:

$$u_C = -kx_S - \left[s^T B\right]^{-1} \eta sat(\sigma/\Phi_b) \quad [40]$$

The gain vector *k* can be calculated in Matlab using the pole placement method. Figure 3 represents the Simulink diagram of a conventional sliding mode controller for the dynamics of raising sunken vessels.

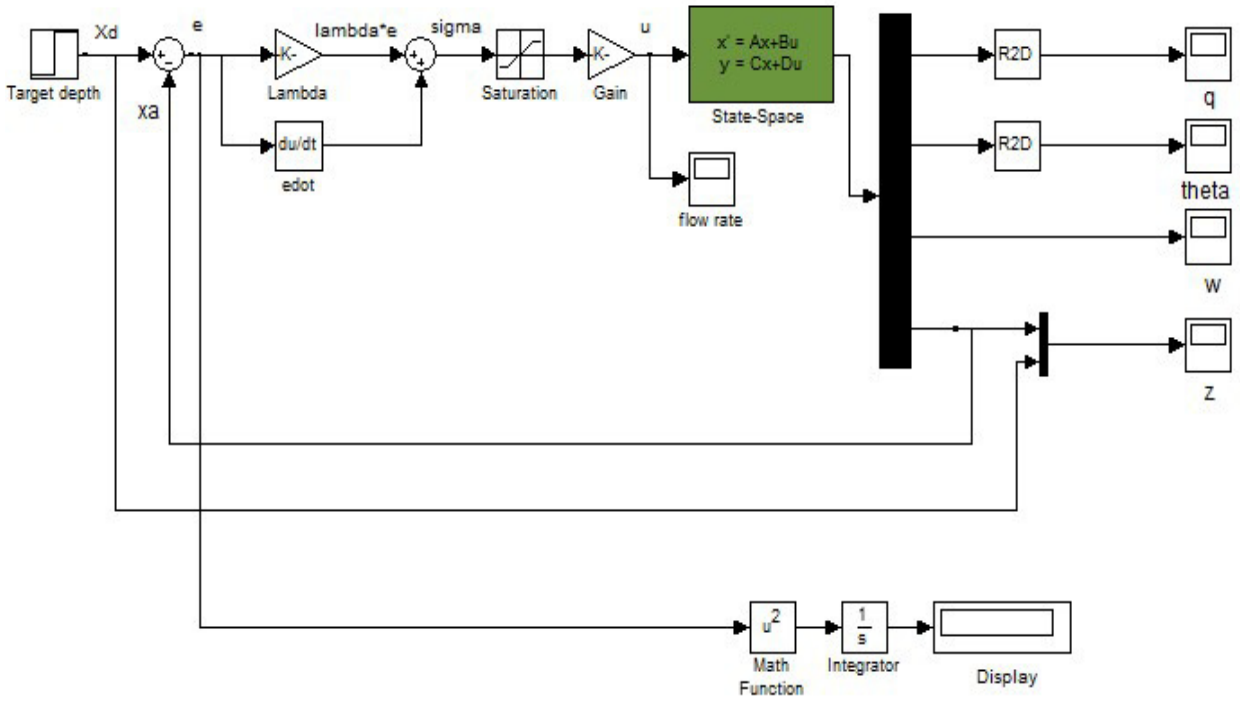

Figure 3: Simulink block diagram of the Conventional Sliding Mode Controller (CSMC) for marine salvage

Design of Conventional (Two Input) Fuzzy Sliding Mode Controller (CFSMC or TIFSMC)

In this section, the performance of the conventional sliding mode controller is improved by using two conventional (two input) fuzzy logic controllers TIFLC1 and TIFLC2, as shown in Figure 4. The first TIFLC1 is used for computing the slope of the sliding surface dynamically according to the system states such as error and change in error so that the tracking performance can be improved, thus maintaining the robustness throughout the process. The second TIFLC2 then calculates the controller gain adaptively with respect to the sliding surface σ and its derivative $\dot{\sigma}$, thereby eliminating the complex process of tuning and reduces chattering.

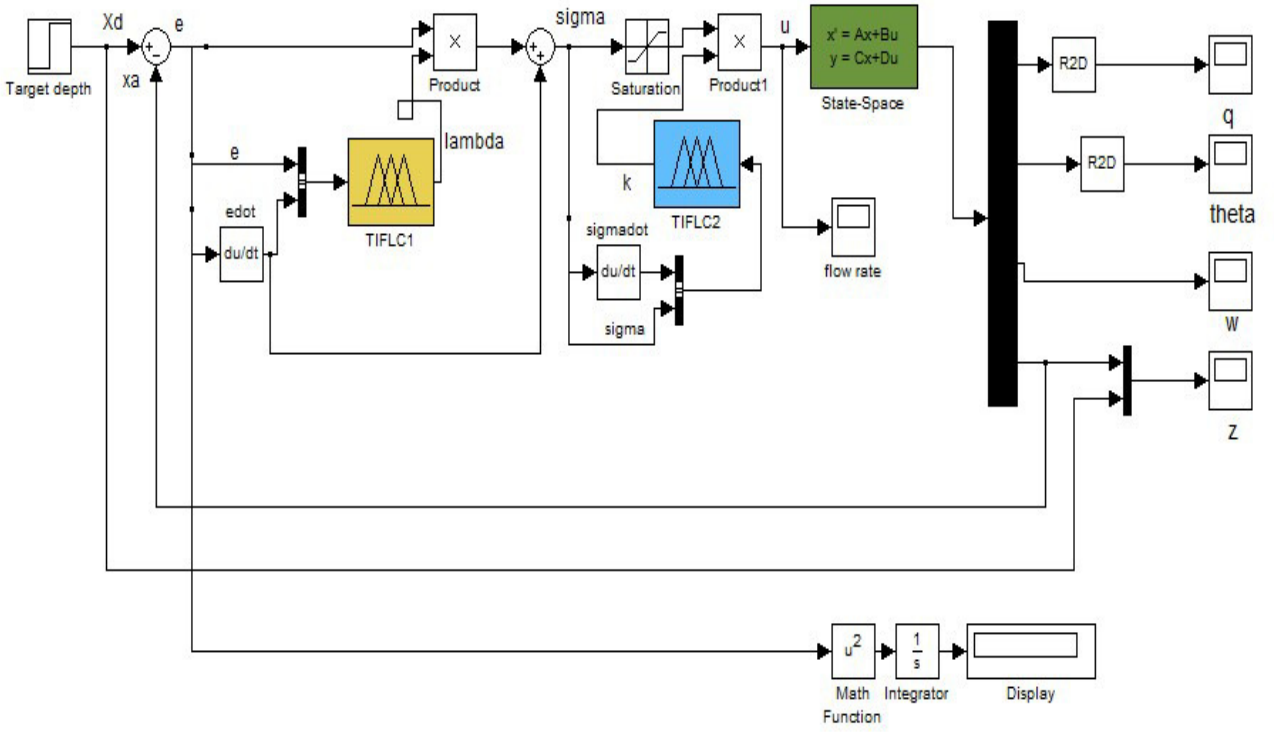

Figure 4: Simulink block diagram of a Conventional or Two Input Fussy Sliding Mode Controller (CFSMC or TIFSMC)

TIFLC1 computes the value of λ dynamically based on the system error (e) and change of error ($\dot{e}$) so that the tracking performance of the system can be improved. The combination of trapezoidal and triangular membership functions are used for modelling the input variables e & $\dot{e}$ as shown in Figures 5(a) and (b), respectively. The shapes of all membership functions for the output λ are chosen being triangular, fully-overlapping and fully-symmetric, as shown in Figure 5(c). Seven linguistic sets have been chosen as NB, NM, NS, ZE, PS, PM, PB for the inputs and VVS, VS, S, M, B, VB, VVB for the outputs, where the abbreviations N stands for negative, P positive, ZE zero, B big, M medium, S small and V very, respectively. It is assumed that the input variables are normalized within a universe of discourse (UOD) of [-1 1] during the process of fuzzification (Palm, et al 1997). Two dimensional fuzzy rules for computing λ are created based on the work of Yorgancioglu & Komurcugil (2010) whereby the values of λ are always positive in order to satisfy the stability condition. These seven linguistic sets lead to 49 fuzzy rules as shown in Table 1. Figure 6 graphically represents the input-output relation or the fuzzy control surface of TIFLC1.

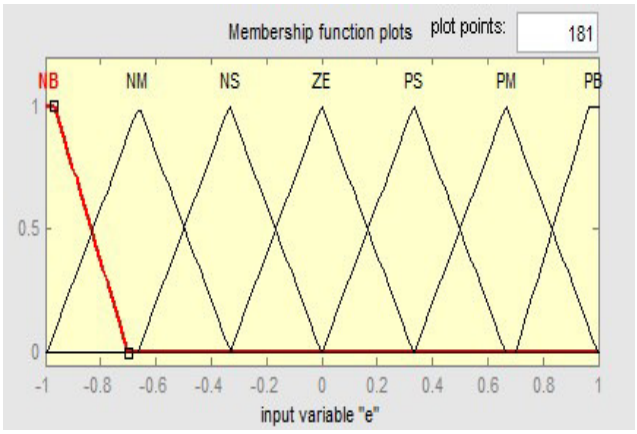

(a)

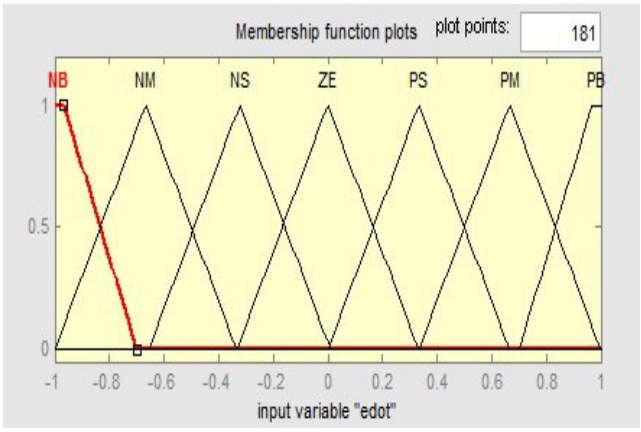

(b)

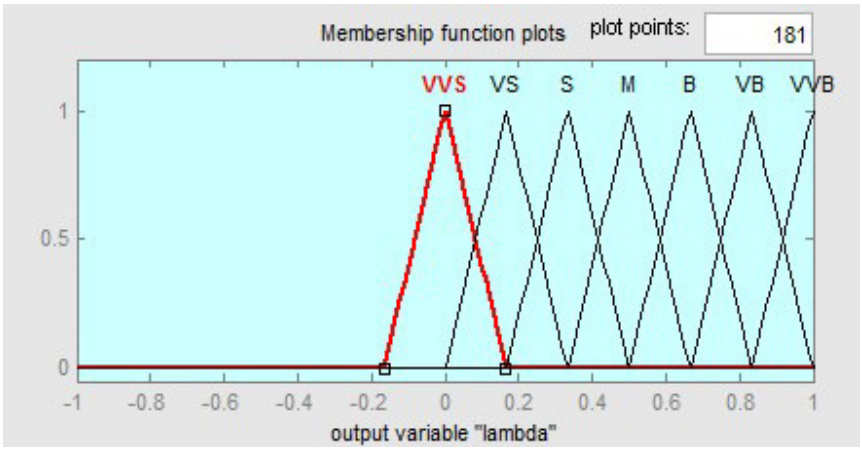

(c)

Figure 5 (a) & (b): TIFLC 1 input membership functions (c): output membership functions

Table 1: Two- dimensional fuzzy rule table to compute λ

e(t)	*ė(t)*						
	NB	**NM**	**NS**	**ZE**	**PS**	**PM**	**PB**
NB	**M**	**S**	**VS**	**VVS**	**VS**	**S**	**M**
NM	**B**	**M**	**S**	**VS**	**S**	**M**	**B**
NS	**VB**	**B**	**M**	**S**	**M**	**B**	**VB**
ZE	**VVB**	**VB**	**B**	**M**	**B**	**VB**	**VVB**
PS	**VB**	**B**	**M**	**S**	**M**	**B**	**VB**
PM	**B**	**M**	**S**	**VS**	**S**	**M**	**B**
PB	**M**	**S**	**VS**	**VVS**	**VS**	**S**	**M**

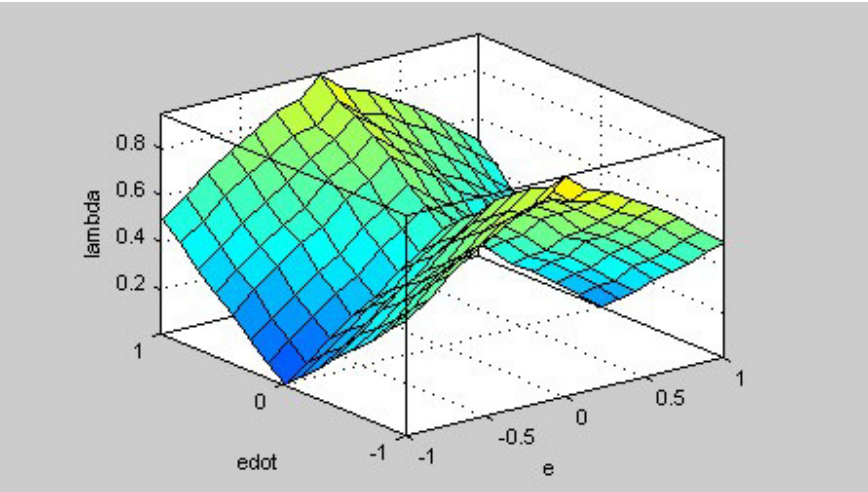

Figure 6: Input- output relation or fuzzy control surface

The controller TIFLC2 computes the controller gain dynamically based on the sliding surface σ and its derivative $\dot{\sigma}$ by which chattering can be avoided. For simplicity, the triangular, fully overlapping and fully symmetrical membership functions are used for representing the input/output variables. Fuzzy rules are selected in such a way that the control gain k is always maintained to positive values in order to satisfy the Lyapunov stability condition as shown in Table 2. Figure 7 shows the three dimensional representation of the input-output relation or the fuzzy control surface of TIFLC2.

Table 2: Two dimensional fuzzy rules to compute k

$e(t)$	$\dot{e}(t)$						
	NB	**NM**	**NS**	**ZE**	**PS**	**PM**	**PB**
NB	**M**	**B**	**VB**	**VVB**	**VB**	**B**	**M**
NM	**S**	**M**	**B**	**VB**	**B**	**M**	**S**
NS	**VS**	**S**	**M**	**B**	**M**	**S**	**VS**
ZE	**VVS**	**VS**	**S**	**M**	**S**	**VS**	**VVS**
PS	**VS**	**S**	**M**	**B**	**M**	**S**	**VS**
PM	**S**	**M**	**B**	**VB**	**B**	**M**	**S**
PB	**M**	**B**	**VB**	**VVB**	**VB**	**B**	**M**

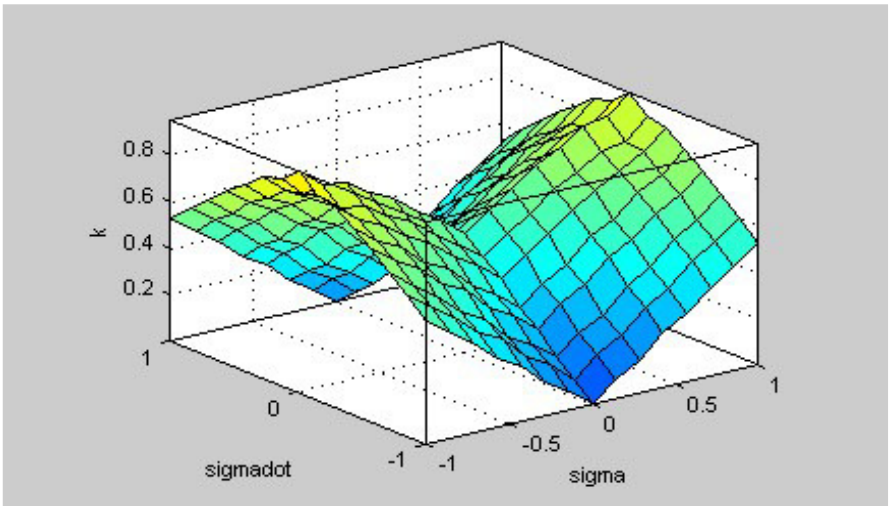

Figure 7: Input- output relation or fuzzy control surface

Design of Single Input Fuzzy Sliding Mode Controller (SIFSMC)

Design procedure of the CFSMC or TIFSMC is complicated due to the involvement of large number of fuzzy rules and parameters to be tuned. The TIFSMC requires the process of fuzzification, rule inferences, defuzzification process that involved extensive computation which leads to the requirement of high performance computing. As a remedy to this problem, a SIFSMC is designed recently to reduce the large number of fuzzy rules, hence minimum computational time and less tuning effort (Yorgancioglu & Komurcugil 2008; Choi et al 1999). The SIFSMC allows the control surface to represent in a 2-D form, i.e. approximation as a linear or piecewise linear surface irrespective of the 3-D surface by which the number of tuning parameters can be considerably reduced. In the SIFSMC, the single fuzzy input variable (e_d) is defined as the absolute magnitude difference between the state error (e) and its derivative (e_{dot}) (Yorgancioglu & Komurcugil 2008).

$$e_d(t) = \left| e(t) - \dot{e}(t) \right| \qquad [41]$$

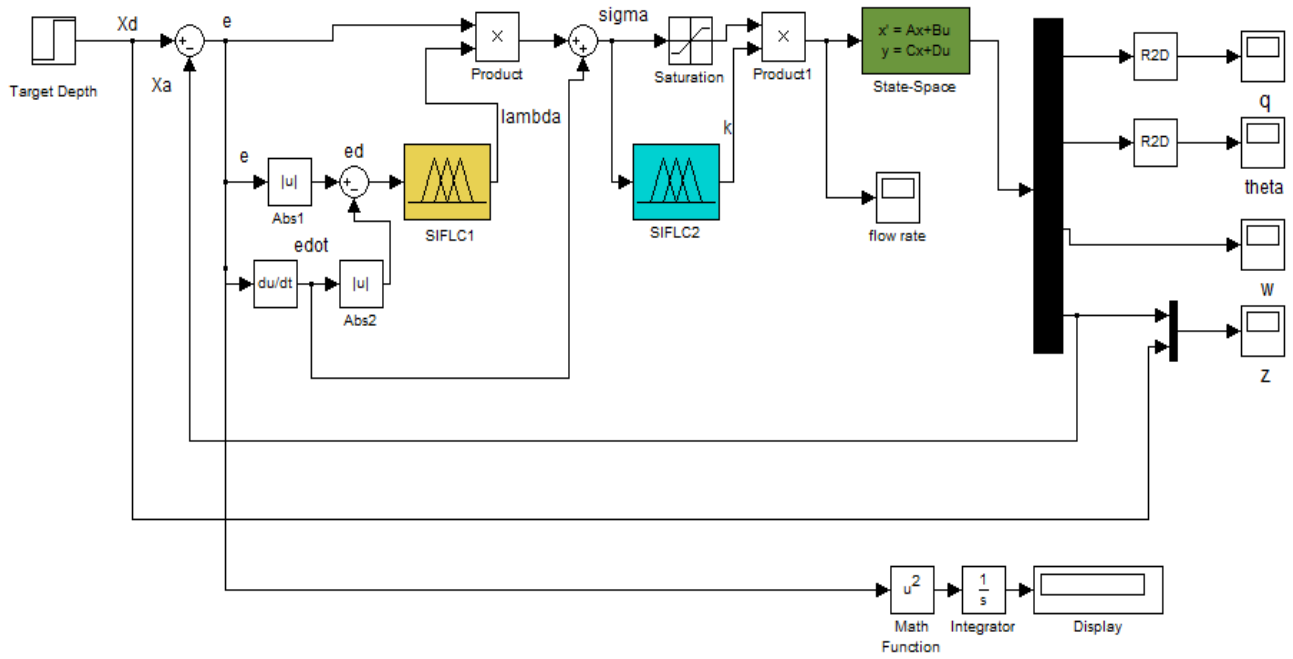

Figure 8: Simulink block diagram of a Single Input Fussy Sliding Mode Controller (SIFSMC)

The SIFLC1 dynamically computes the sliding surface slope based on the absolute magnitude difference between the state error e and its derivative $\dot{e}$. Similar to the previous case, both the triangular and trapezoidal membership functions are used for modelling the input variable e_d, while the triangular membership functions are used for representing the output λ. One dimensional fuzzy rules are formulated based on the work of Yorgancioglu & Komurcugil (2008). Table 3 shows that the fuzzy rules are considerably reduced from 49 to 7 in comparison with the TIFLC1. As it is a single input-output system, the input-output relation can be approximated as a straight line as shown in Figure 9.

Table 3: One dimensional fuzzy rules to compute λ

Rule No	One dimensional fuzzy rules
1	If (e_d is NB) then (λ is VVB)
2	If (e_d is NM) then (λ is VB)
3	If (e_d is NS) then (λ is B)
4	If (e_d is ZE) then (λ is M)
5	If (e_d is PS) then (λ is S)
6	If (e_d is PM) then (λ is VS)
7	If (e_d is PB) then (λ is VVS)

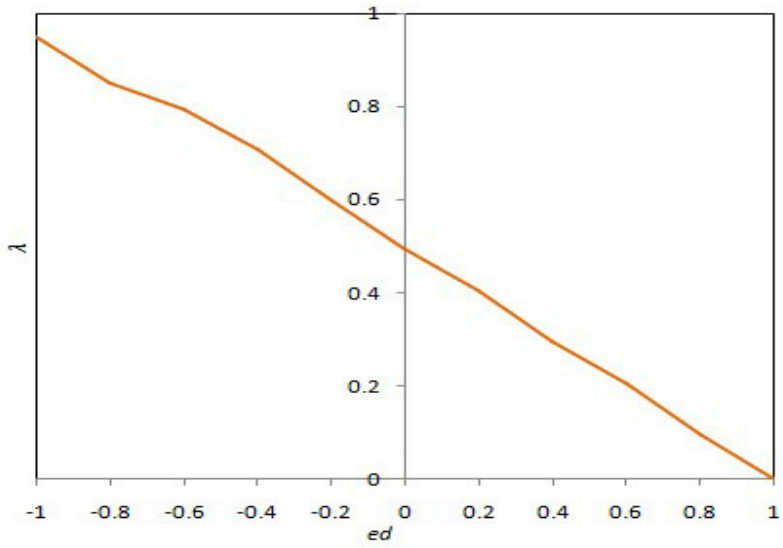

Figure 9: Input- output relation or control surface.

The fuzzy logic controller SIFLC2 computes the controller gain adaptively based on the sliding surface σ. The triangular, fully symmetrical and fully overlapping membership functions are used for modeling both input and output variables. Table 4 represents the 1-D fuzzy rule table to compute the gain k. Figure 10 represents the fuzzy control surface.

Table 4: One dimensional fuzzy rules to compute k

Rule No	One dimensional fuzzy rules
1	If (σ is NB) then (k is VVS)
2	If (σ is NM) then (k is VS)
3	If (σ is NS) then (k is S)
4	If (σ is ZE) then (k is M)
5	If (σ is PS) then (k is B)
6	If (σ is PM) then (k is VB)
7	If (σ is PB) then (k is VVB)

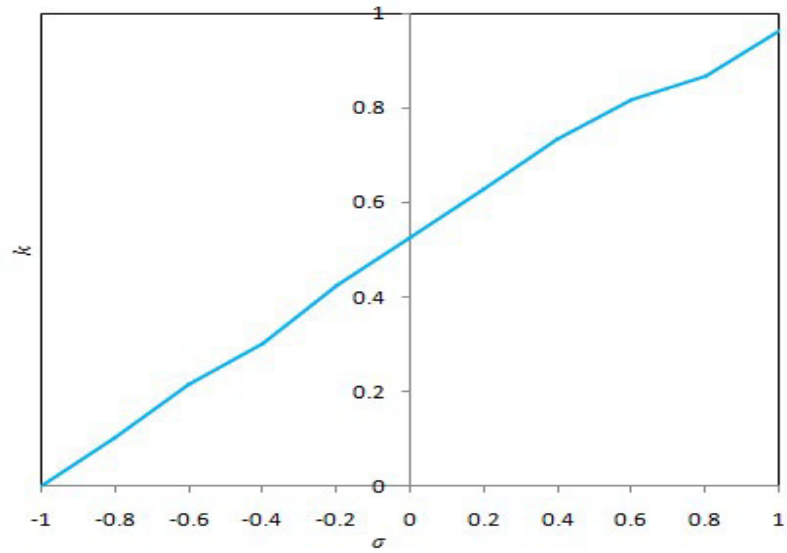

Figure 10: Input- output relation or fuzzy control surface

NUMERICAL RESULTS AND DISCUSSION

Numerical simulations based on a small-scale pontoon model have been carried out using Matlab & Simulink. This model with the gas-inflated balloons will be tested at sea in the mid-2012. The pontoon is a rectangular-shaped structure with watertight compartments for internal deployment of balloons and gas generating system. The balloon length is 1.8 m and the maximum space in a single compartment for the installation of a gas generator including piping is 0.29 m in diameter and 2 m in length (Susy 2011). Figure 11 exemplifies the installation of inflating system inside a single pontoon compartment.

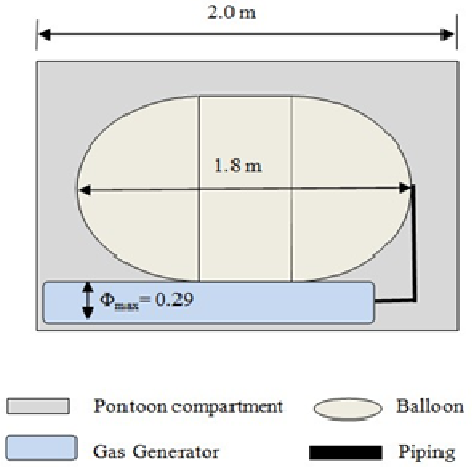

Figure 11: Pontoon compartment with inflating system (Susy 2011)

Table 5: Input parameters in the simulation program

Parameters	Values & Units
W	9320 kg
l	6.0 m
b	3.0 m
ρ	1025 kgm^{-3}
ρ_g	1.017 kgm^{-3}
I_{yy}	1481.31 kgm^2
$Z_{\dot{w}}'$	- 15.7x 10^{-3}
$Z_{\dot{q}}'$	- 0.41x10^{-3}
$M_{\dot{w}}'$	- 0.53x10^{-3}
$M_{\dot{q}}'$	- 0.79x10^{-3}

Table 5 shows the input physical and empirical parameters for the pontoon model. Simulation is carried out for a target depth of 50 m. The minimum volume of gas required for lifting the pontoon model to 50 m is calculated based on basic hydrostatic principles and it is found to be 15 m^3 .The initial flow rate of filling gas inside the balloon is selected as 0.25 m^3s^{-1} so that the inflation time is 60 sec. Total lift force required to extract the pontoon from sea bottom is 1.3 times the wet weight, which is found to be 103341.68 N (of the order of 10^5). According to Foda (1982), for the estimated break out force, the break out time can be obtained as 100 sec. The obtained vertical dynamic responses (vertical trajectory, ascent velocity, pitch angle

and pitch rate) and the variation of the control parameter (i.e. the flow rate) are presented in Figures 12-15 and Figure 16, respectively.

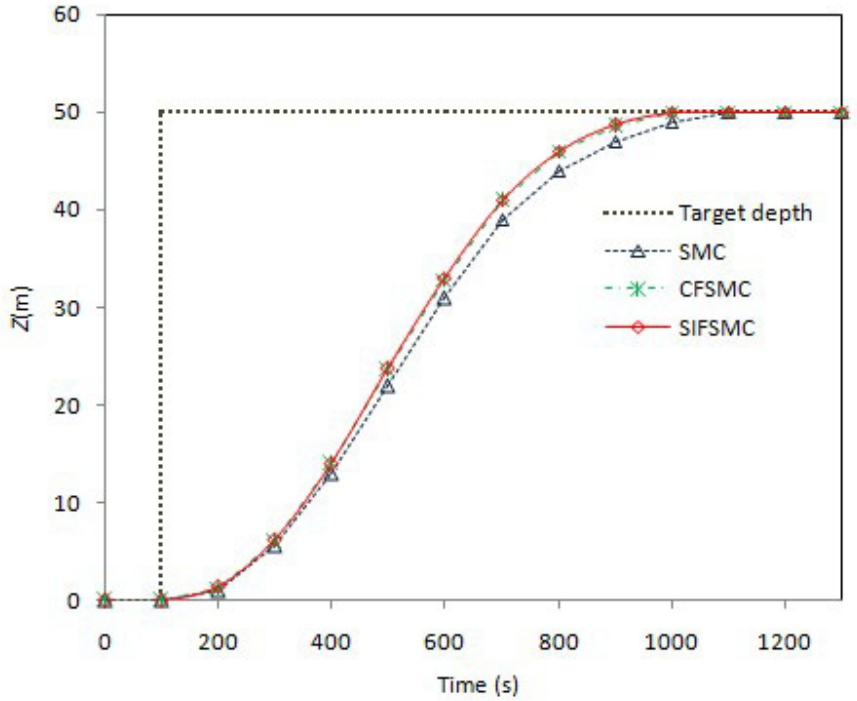

Figure 12: Variation of ship vertical position

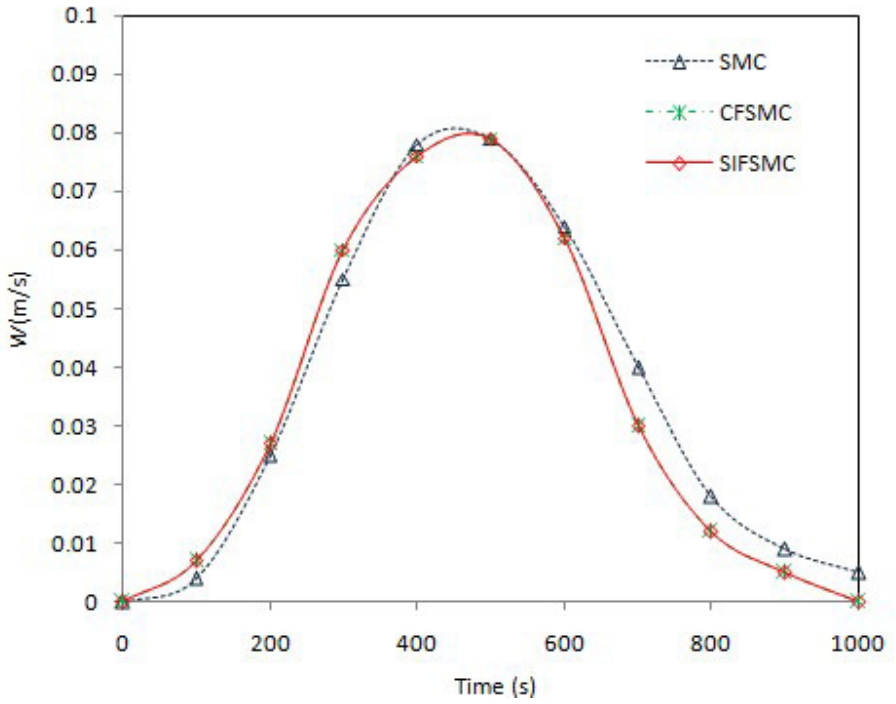

Figure 13: Variation of ship ascent velocity

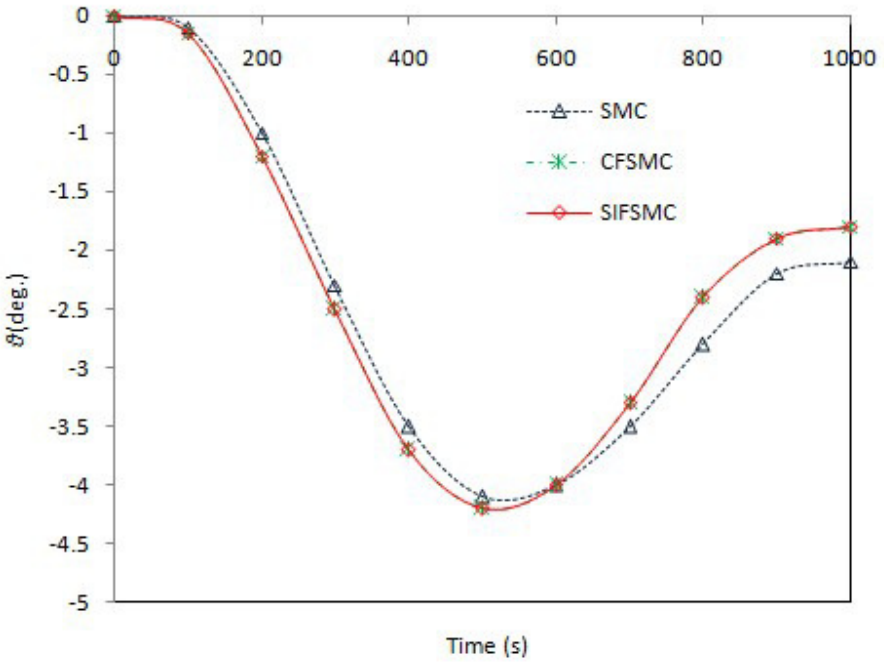

Figure 14: Variation of ship pitch angle

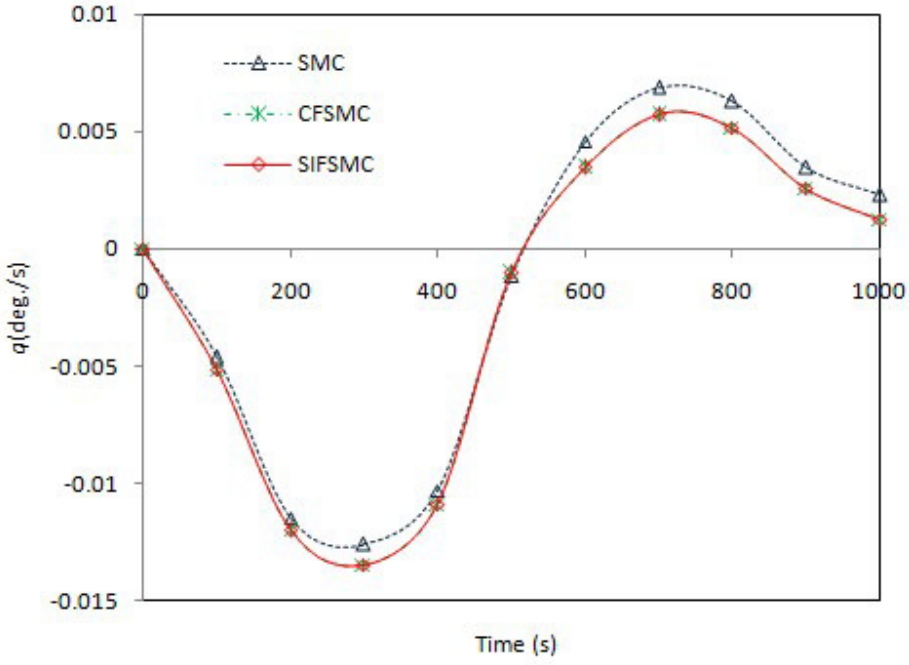

Figure 15: Variation of ship pitch rate

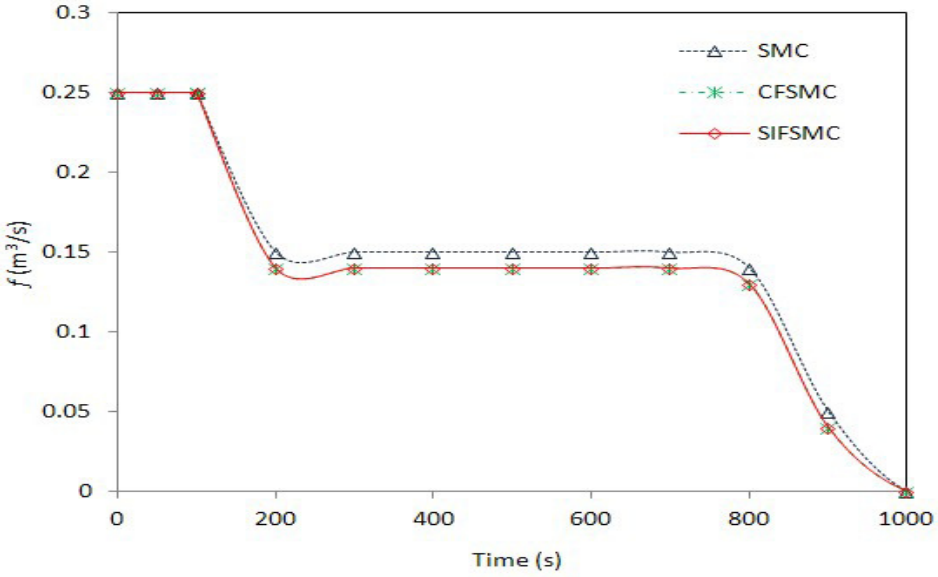

Figure 16: Variation of gas flow rate

In all cases, the responses obtained from conventional SMC and FSMC are nearly same. From Figure 12, it is seen that the payload reaches the target depth within 1000 sec (17 minutes), which entails a comparatively slow process. It is seen from Figure 13 that the heave velocity (ascent velocity) increases with time, reaches a maximum value and then starts decreasing. The maximum value of the ascent velocity is found to be 0.08 m/s - being within the required range (< 0.6 m/s; J W Automarine 2010). This implies how the pontoon motion is stable. When the vessel reaches the commanded depth, the controller reduces the ascent velocity to the nearly-zero value. The depth rate and ascent velocity responses reveal similar trend to the results of Nicholls-Lee et al. (2009). From Figure 14, the pitch angle is found to increase with time, reaching a maximum value during a half of period and thereafter decreasing. The maximum value of the pitch angle is found to be about 4.2 deg. which is within the required limit (< 15 deg; J W Automarine 2010). The pitch angle decreases when the payload reaches the commanded depth due to the fact that the controller generates a pitch angle command as per the depth error. At the beginning, the depth error is large thereby the controller produces a high value of pitch angle to eliminate the error. Figure 15 shows how the pitch rates become nearly equal to zero when the pontoon reaches the required positions. It is seen from Figure 16 that soon after the breaking out period (at t = 100 s) the controller instantly reduces the flow rate value from 0.25 to 0.15 m^3s^{-1} in order to compensate the presence of excessive buoyancy induced by a sudden release of the pay load from the sea bottom. Thereafter, the flow rate of gas filling maintains a constant value until the vessel nearly reaches the target depth. Once the target depth is fulfilled, the controller further reduces the flow rate to almost the zero value. The variation in the buoyancy force with respect to the varying depth is compensated by the pressure relief valves. Thus, by the combined use of an adaptive sliding mode controller for regulating the flow rate of filling and pressure relief valves, a constant and stable ascent rate can be reasonably maintained.

Overall, all three controllers show good performance over the system. When Figure 13 is considered, the slow response of the conventional SMC is improved by continuously varying the sliding surface slope and online tuning the controller gain so that the ascent velocity approaches exact zero value as soon as the pay load reaches the target depth (50 m). The rise time produced by all controller models are nearly the same, but the time required for the state variables to attain the steady state condition is lesser in the FSMC than the conventional SMC. In all cases, the state variables attain their steady state, indicating how the dynamic system is stable throughout the process. The percentage of overshoot is negligible with all controllers. It is observed that fuzzy sliding mode controllers are free from chattering due to high free switching as inherently seen in conventional sliding mode controllers. Since it is difficult to visually observe the comparative performance of these controllers, the Integral Absolute Error (IAE) is considered during the simulations. It is found that both FSMCs show about 30% of improvement in the IAE index compared to the conventional SMCs. In addition, in terms of the transient response, both FSMCs better perform. For the conventional FSMC, the above transient performance is obtained after a lengthy complex tuning process of fuzzification, defuzzification and inference of 49 rules. If these processes had not been properly tuned, unsatisfactory results would have been produced by the CFSMC. Irrespective of the 3D control surface of CFSMC in Figures 6 and 7, SIFSMC requires only two parameters to be tuned; slope of the linear control surface and the break point as shown in Figures 9 and 10. Table 6 shows the computational time required for the two FSMCs. It is seen that SIFSMC is two

orders of magnitude faster than CFSMC. This is due to the reduction in linguistic fuzzy rules from 49 to 7. Finally, it is worth emphasizing that the SIFSMC can be implemented using a much slower and low cost processor with minimum tuning effort.

Table 6: Comparison of computational time

Controller	Computational time (s)
CFSMC	500
SIFSMC	4

CONCLUSIONS

This paper described a mathematical modelling and numerical time-domain approach to simulate the dynamics of a sunken vessel being raised from the seafloor by a gas inflating system. A new controller design is implemented that brings together the advantages of fuzzy logic and sliding mode controller. A conventional sliding mode controller (SMC) is first designed and then its performance is improved by extending to fuzzy SMCs (two-input versus single-input). With the two-input fuzzy SMC, the dynamic sliding surface slope is computed according to system error and its derivative by a two input fuzzy logic controller and the controller gain is adaptively tuned using the system error states via another two input fuzzy logic controller. With the single-input fuzzy SMC, single input fuzzy logic controllers are used for computing the surface slope and gain. The effectiveness of the fuzzy SMCs over the conventional SMC is illustrated by the simulations of an experimental pontoon model. The obtained numerical results highlight that the fuzzy SMCs show 30% of improvement in the tracking performance when compared to the conventional SMC, while maintaining its robustness. The responses obtained by the single-input fuzzy SMC are the same as those obtained by the conventional (two-input) fuzzy SMC, with the former involving a much less tuning effort and computational time. Therefore, the single-input fuzzy SMC proves to be the preferred option amongst the considered controllers.

ACKNOWLEDGEMENT

This work is part of the SuSy (Surfacing System for Ship Recovery) project funded by the European Commission FP7 framework (www.su-sy.eu). We are very grateful for this support.

REFERENCES

ABDELHAMEED, M.-M., “Enhancement of sliding mode controller by fuzzy logic with applications to robotic manipulators”, *Mechatronics* 15, pp 439-458, 2005.

BAZZI, B.A., CHALHOUB, N.G., “Fuzzy Sliding mode Controller for a Flexible Single-link Robotic Manipulator” , *Journal of Vibration and Control* 11. pp 295-314, 2005.

CHOI, B.J., KWAK, S,W., KIM, B.K., “Design of a single input fuzzy logic control & its properties”, *Fuzzy Sets and Systems*, 106 (3), pp 299-308, 1999.

CRISTI,R., PAPOULIAS, F.A., HEALEY, A.J. “Adaptive Sliding Mode Control of Autonomus Under water vehicles in the diving plane”. *IEEE Journal of Ocean Engineering*, Vol. 15, No.3, July 1990.

EKSIN, I., GUZELKAYA, M., TOKAT, S., “Self tuning mechanism for sliding surface slope adjustment in fuzzy sliding mode controllers”, Proceedings of the Institution of Mechanical Engineers, Part 1: Journal of Systems and Control Engineering, pp 216-393, 2002.

FARREL,J.& WOOD, S. “An Automatic Purge Valve for Marine Salvage”, *IEEE Conference,* New Jersey, 2009.

FODA, M.A., “On the Extrication of large objects from the ocean bottom (the breakout phenomenon)”, Journal of Fluid Mechanics, Vol.117, pp. 211-231,1982.

FOSSEN, T,I., “Guidance and Control of Ocean vehicles” , Wiley , Newyork, 1994.

FOSSEN, T.I., “Marine Control Systems – Guidance , Navigation and Control of Ships, Rigs and Underwater Vehicles”. Marine Cybernetics, Trondheim, Norway, 2002.

GUO,Y., WOO, P.-Y., "An Adaptive Fuzzy Sliding Mode Controller for Robotic Manipulators", IEEE Transactions on Systems, Man and Cybernetics- Part A: Systems and Humans, vol 33. No.2. March 2003.

HEALEY, A.J.,& LIENARD ,D.,"Multivariable sliding mode control for autonomus diving and steering of unmanned underwater vehicles"., *IEEE Journal of Oceanic Engineering*, 18(3), 327-339, 1993.

HEALEY , A.J., & MACRO,D.B., "Slow speed fight control of autonomus under water vehicles experimental results with NPS AUV II", *Proceedings of The 2nd International Offshore & Polar Engineering Conference*, pp. 523- 532., 1992.

HUANG, L.C., LIN, H.P., CHUNG,H.Y., "Design of self tuning fuzzy sliding mode control for TORA system", *Expert Systems with Applications 32,* pp 201- 212, 2007.

J W Automarine, "The theory of lifting bags". Retrieved on Oct. 4, 2010, www.jwautomarine.co.uk.

MCGOOKIN , E.W., "Optimisation of sliding mode controllers for marine applications: a study of methods and implementation issues". PhD thesis, University of Glasgow, 1997.

MCGOOKIN, E.W., MURRAY-SMITH, D.J., "Submarine manoeuvring controller's optimisation using simulated annealing and genetic algorithms". *Control Engineering Practice 14* , 1-15, 2006.

MEI,C.C., Yeung, R.W. & Liu, K.F., "Lifting of a Large Object from a Porous Seabed", Journal of Fluid Mechanics, Vol.152, pp. 203-215,1985.

NICHOLLS-LEE, R.F., TURNOCK ,S.R., TAN, M., MCDONALD, P,C.,SHENOI, R.A.,"Use of cryogenic buoyancy systems for controlled removal of heavy objects from sea bottom", *Proceedings of the ASME 28th International Conference on Ocean ,Offshore & Arctic Engineering*, 2009.

PALM, R., DRIANKOV,D., HELLENDOORN, H., "Model Based Fuzzy Control" , Springer-Verlag, Germany, 1997.

RAWSON, K.J. & TUPPER, E, C., "Basic Ship Theory - Vol. 1", Fifth Edition. Butterworth-Heinemann publishing, Oxford, 2001.

SAWICKI,A., MIERCZYNSKI,J., "Mechanics of breakout phenomenon", *Computers and Geotechnics 30* , pp 231-243, 2003.

SLOTINE, J.J.E., & LI,W., 'Applied non- linear control', NJ,USA, 1991.

"SuSy project mid-term report", 2011.

U.S. NAVY, "Salvage Engineer's Handbook", Volume1, 1992.

VAUDREY, K.D., "Evaluation of bottom breakout reduction methods", Technical Note N-1227, Naval Civil Engineering Laboratory, Port Huneme, Ca, 1972.

VELAYUDHAN, A K D., SRINIL, N., BARLTROP, N., "Sliding Mode Controller for Salvaging of Sunken Vessels", *Proceedings of RINA 15th International Conference on Computer Applications in Ship Building*, Trieste, Italy, 2011.

YAGIZ,N., HACIOGLU,Y.,"Fuzzy Sliding Modes with Moving Surface for the Robust Control of a Planar Robot".*Journal of Vibration and Control* 11, pp 903-922, 2005.

YOERGER, D.R., SLOTINE, J.J.E., "Robust trajectory control of underwater vehicles", *IEEE J. Oceanic Eng*., vol. 10, pp. 462-470, Oct.1985.

YORGANCIOGLU, F., KOMURCUGIL, H.,"Single-input fuzzy-like moving sliding surface approach to the sliding mode control", *Electl Engg* 90, pp 199- 207, 2008.

YORGANCIOGLU, F., KOMURCUGIL, H., "Decoupled sliding mode controller based on time- varying sliding surfaces for fouth-order systems" , *Expert Systems with Applications 37,* pp 6764- 6774, 2010.